Confinement of Acoustical Vibrations in a Semiconductor Planar Phonon Cavity

M. Trigo,[1] A. Bruchhausen,[1] A. Fainstein,[1] B. Jusserand,[2] and V. Thierry-Mieg[2]
[1]*Centro Atómico Bariloche & Instituto Balseiro, C.N.E.A., 8400 San Carlos de Bariloche, Argentina*
[2]*Laboratoire de Photonique et de Nanostructures, CNRS, Route de Nozay, 91460 Marcoussis, France*
(Received 3 June 2002; published 11 November 2002)

Extending the idea of optical microcavities to sound waves, we propose a *phonon cavity* consisting of two semiconductor superlattices enclosing a spacer layer. We show that acoustical phonons can be confined in such layered structures when the spacer thickness is an integer multiple of the acoustic half-wavelength at the center of one of the superlattice folded minigaps. We report Raman scattering experiments that, taking profit of an optical microcavity geometry, demonstrate unambiguously the observation of a phonon-cavity confined acoustical vibration in a GaAs/AlAs based structure. The experimental results compare precisely with photoelastic model calculations of the Raman spectra.

DOI: 10.1103/PhysRevLett.89.227402 PACS numbers: 78.30.Fs, 42.60.Da, 63.20.Dj, 78.66.Fd

A planar periodic stack of two materials of contrasting refractive index and thickness $\lambda/4$ reflects photons propagating normal to the layers within a stop band around the wavelength λ, and is termed a "Bragg reflector" (BR). A microcavity is a spacer of thickness $\lambda/2$ enclosed by two BR's [1]. Photons of wavelength λ are confined in such structure, leading to fundamental changes in the light-matter interaction [1]. We have shown that this photon confinement can be exploited, for instance, to obtain hugely enhanced ($\times 10^5$) Raman cross sections in double optical resonant geometries [2]. Such Raman scattering geometries have lead to novel phonon physics, including the observation of standing optical phonons in finite-size multiple quantum wells [3].

Acoustical phonons are vibrational waves described by similar wave equations as photons, but which are subject to mechanical (instead of electromagnetic) boundary conditions at the interfaces. Extending these ideas from photon confinement to confinement of vibrational waves, we propose a planar "phonon cavity" structure designed to confine acoustical phonons. In addition, we show theoretically that Raman scattering through an optical cavity geometry [2,3] is able to probe these novel excitations, and we demonstrate their existence through experiments in a real GaAs/AlAs based structure. These results are relevant to diverse phenomena as, e.g., phonon amplification and stimulated emission [4–6], coherent generation and control of phonons [7], and modified electron-phonon interactions.

The acoustical phonon branches in a superlattice (SL) made of a periodic sequence of semiconductor layers can be described by backfolding the phonon dispersion of an average bulk solid and opening of small minigaps at the zone center and reduced new Brillouin-zone edge [8]. It was proposed a long time ago that the minigap of these zone-folded SL acoustical phonons could be used as a "phonon filter," acting very much like dielectric BR's but for the selective reflection of high frequency sound waves [9,10]. Thus, a planar phonon cavity can be constructed by enclosing between two SL's a spacer of thickness equal to an integral number of $\lambda_{ac}/2$, where now λ_{ac} is the wavelength of the acoustical phonon at the center of the phonon minigap. In Fig. 1 we present a scheme of the proposed phonon-cavity structure, based in semiconductor GaAs and AlAs materials. The "phonon BR's" consist of 11 period 74 Å/38 Å GaAs/AlAs SL's, and enclose a 50 Å $Al_{0.8}Ga_{0.2}As$ spacer.

The acoustical phonons in the proposed layered structure can be evaluated using a matrix method implementation of the standard elastic continuum description of sound waves originally proposed by Rytov [8]. With this model one can obtain the transmission of acoustical waves through the structure, and the displacement pattern as a function of the phonon energy. In Fig. 2 (top) we

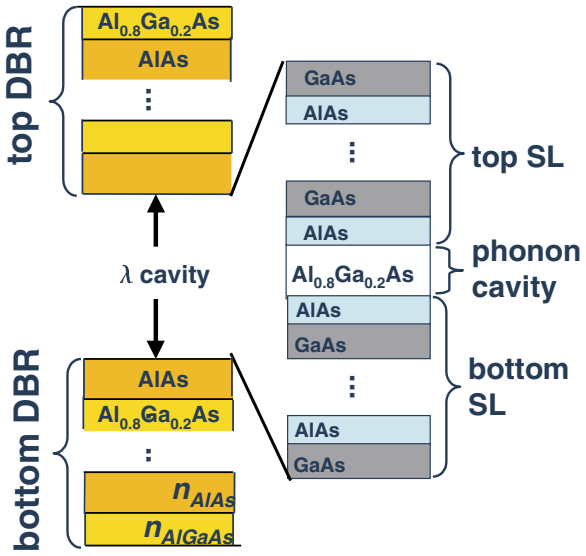

FIG. 1 (color online). Scheme of the proposed phonon cavity embedded within an optical cavity. The phonon "mirrors" consist of 11 period 74 Å/38 Å GaAs/AlAs SL's, and enclose a 50 Å $Al_{0.8}Ga_{0.2}As$ spacer. The phonon-cavity structure, on the other hand, constitutes the λ spacer of an optical microcavity enclosed by 20 BR $Ga_{0.8}Al_{0.2}As$/AlAs pairs on the bottom and 16 on top.

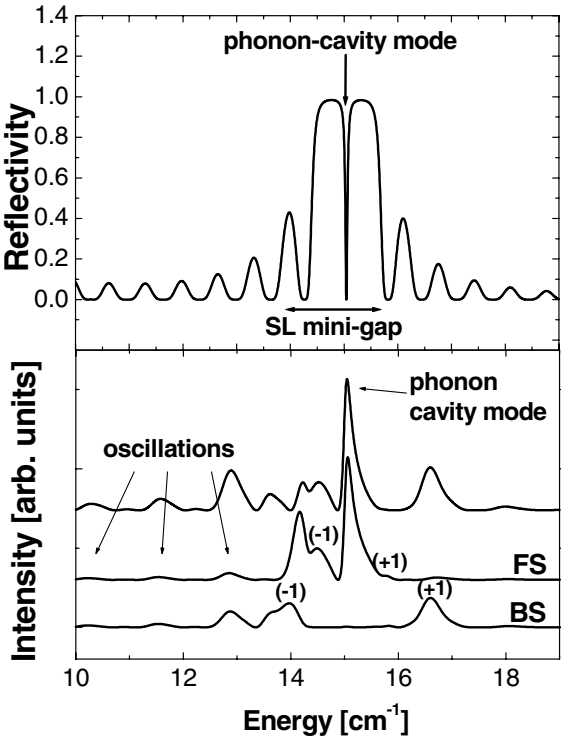

FIG. 2. Calculated phonon reflectivity (top) and Raman spectrum (bottom) in the spectral region around the first zone-center minigap for the phonon cavity embedded within a photon cavity depicted in Fig. 1. The separate contributions of the forward scattering (FS) and backscattering (BS) terms is also shown.

display the calculated phonon reflectivity for energies around the first zone-center minigap. For this calculation standard material parameters (sound velocities and densities) were used [11]. A phonon-transmission stop band is observed, coincident with the SL's minigap. Within this stop band a phonon-cavity mode exists, characterized by complete transmission of the vibrational energy. The calculated phonon amplitude for this latter mode is shown in Fig. 3. While phonon modes with energies within the SL's minigap decay exponentially in space, the phonon-cavity mode propagates through the structure, and its intensity is enhanced within the cavity spacer.

The design of the phonon cavity deserves some consideration. In principle, any of the acoustical minigaps can be used as phonon BR. The center of the phonon stop band (and hence the energy of the confined mode) is simply determined by the SL's period $d = d_1 + d_2$. The stop-band width, on the other hand, is proportional to a modulation parameter ϵ and displays an oscillatory behavior as a function of the SL layers thickness ratio d_1/d_2 [8]. Here $\epsilon = (\eta_2 - \eta_1)/(\eta_1\eta_2)^{1/2}$, with $\eta_i = \rho_i v_i$, ρ_i and v_i the acoustic impedance, density, and sound speed of layer i, respectively. The oscillatory function, and thus the thickness ratio d_1/d_2 maximizing the stop band of the BR's of a phonon cavity, depends also on

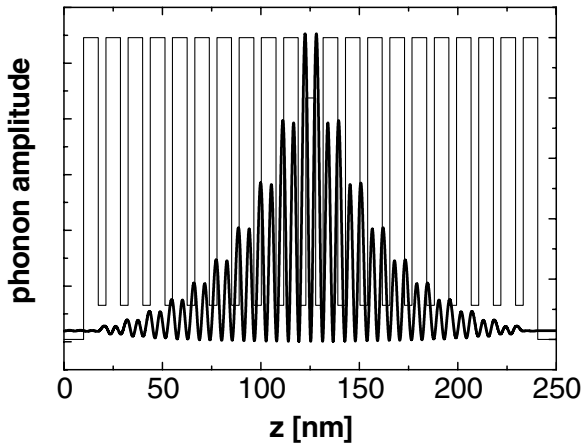

FIG. 3. Calculated phonon amplitude corresponding to the confined phonon-cavity mode. The curve is shown superimposed to a scheme of the phonon structure characterized by the material's photoelastic constant.

the order of the minigap ν. For the first zone-edge minigap ($\nu = 1$) the cavity is optimized using $d_1/v_1 = d_2/v_2 = d_c/2v_c$, while for the first zone-center minigap ($\nu = 2$) the relation is $d_1/v_1 = d_2/3v_2 = d_c/2v_c$. Here $d_c(v_c)$ is the cavity thickness (sound velocity). These expressions can be directly transferred to optical waves by replacing the acoustic impedances in ϵ by the refractive indices n_i. In fact, for GaAs and AlAs it turns out that ϵ has the same magnitude for phonons and photons (0.18 and 0.175, respectively), implying that similar BR reflectivities and cavity Q factors can be obtained as a function of the number of BR layers (N). For our phonon cavity, designed to operate at the first zone-center minigap with 11 SL periods, $Q \sim 140$. On the other hand, Q factors in the range $Q > 3000$ could be obtained with $N \sim 20$.

The issue we address next is how to study the confined vibrational excitations in phonon cavities. As derives from Fig. 2, we require a technique able to resolve $\sim 0.1\ \mathrm{cm}^{-1}$ (i.e., 10^{-2} meV) in the energy range ~ 5–$30\ \mathrm{cm}^{-1}$ (1–4 meV). We propose Raman experiments based in a planar microcavity scattering geometry that, besides providing the required resolution [8] and an amplified efficiency ($\sim \times 10^5$) [2,3], give access to the zone-center excitations through a wave vector conserving contribution. As we will show next, these singular characteristics allow the observation of these novel acoustical phonon excitations.

We consider a phonon cavity embedded within an optical microcavity as depicted in Fig. 1. We have performed calculations of the Raman spectra of the proposed structure based on a photoelastic model for the Raman efficiency. Within a photoelastic model for scattering by longitudinal acoustic phonons the Raman efficiency is given by $I(\omega_{q_z}) \propto |\int dz E_L E_S^* p(z)[\partial\Phi(z)/\partial z]|^2$, where E_L (E_S) is the laser (scattered) field, $p(z)$ is the spatially

varying photoelastic constant, and Φ describes the (normalized) phonon displacement [8]. For an infinite periodic SL the wave vector q_z is a good quantum number. For a standard Raman scattering geometry, with laser and scattered fields given by plane waves [$E_L E_S^* = e^{i(k_L - k_S)z}$], $I(\omega_{q_z})$ leads to the usual phonon doublets with transferred wave number given by the conservation law $q_z = k_L - k_S$. For the case we are discussing, however, q_z is only partially conserved due to the finite size of the structure [2,12]. In addition, E_L and E_S correspond to the cavity-confined photons. Under double optical resonance conditions (that is, both laser and Stokes fields resonant with cavity modes) [2], the incident and scattered photon fields are given within the optical cavity spacer by the same standing wave $E_L = E_S = e^{ik_z z} + e^{-ik_z z}$ (here, by construction, $k_z = \pi/D$ with D the spacer width) [3]. Consequently, $E_L E_S^* \propto |E(z)|^2 = 2 + (e^{i2k_z z} + e^{-i2k_z z})$. Thus, both a wave vector conserving (the term 2) and a wave vector modulating contribution ($e^{i2k_z z} + e^{-i2k_z z}$) are coherently added to the Raman efficiency $I(\omega_{q_z})$. The latter leads to a wave vector transfer $q_z = 2\pi/D$ and corresponds to the standard backscattering (BS) Raman signal [8]. On the other hand, $q_z = 0$ for the wave vector conserving term which could be, in principle, accessed by a forward scattering (FS) geometry in an optically nonconfined structure.

We show in Fig. 2, together with the phonon reflectivity curve, a calculated Raman spectrum for the phonon cavity embedded photon cavity of Fig. 1. For this calculation the laser wavelength is $\lambda = 833$ nm, the layers refractive indices $n_{\mathrm{GaAs}} = 3.56$ and $n_{\mathrm{AlAs}} = 2.97$ and, being λ in the transparency region, the photoelastic constants are taken real [8,11]. For discussion purposes we also present, in the bottom panel, the separate contributions of the FS ($q_z = 0$) and BS ($q_z = 2\pi/D$) terms. Note that the main Raman peak in Fig. 2 corresponds to scattering by the phonon-cavity confined mode. Interestingly, this latter feature comes *only* from the FS (wave vector conserving) contribution. Its relatively large intensity is explained by the spatial confinement of the cavity-phonon mode at the same place where the confined cavity *photon* has the largest amplitude. In addition, several other features should be noted in the calculated spectra: (i) besides the confined phonon mode, the FS contribution displays scattering at the low energy side of the minigap, corresponding to the (-1) zone-center SL folded minigap mode [8]. The ($+1$) peak is forbidden in an infinite SL due to a parity selection rule [8], and is only weakly perceptible in the shown spectra due to a partial relaxation of q_z conservation due to the phonon cavity SL mirror's finite-size. (ii) The BS contribution, on the other hand, displays the usual SL phonon doublet. (iii) Side oscillations are observed that modulate the spectra. These oscillations originate in the SL's finite size [13,14], and are particularly intense in the cavity spectrum because they add coherently from the BS and FS terms. With "coherence" here we mean that the BS and FS contributions are added *before* (and not after) squaring in $I(\omega_{q_z})$. And last, (iv) the coherent addition of BS and FS in the total cross section is particularly clear around ~ 14 cm^{-1} where the cavity spectrum is not the simple sum of the individual contributions.

With the above Raman calculations in mind we fabricated, using standard molecular beam epitaxy techniques, a phonon cavity embedded within an optical cavity with the structure and nominal layer thicknesses as given in Fig. 1. The structure was purposely grown with a slight taper which enables a tuning of the optical cavity mode by displacing the laser spot on the sample surface. The coupling of both laser and Stokes (nondegenerate) photons with the optical cavity mode is accomplished by tuning the incidence angle as described in Ref. [2]. Since the acoustical folded-phonon-like excitations are in the range 10–30 cm^{-1} (i.e., $\sim$1–4 meV), incidence angles around $\sim 3°$–$5°$ are required. The Raman experiments were performed at 77 K using a triple Jobin-Yvon T64000 spectrometer equipped with a N_2-cooled charge-coupled device. A Ti-sapphire laser was used as the excitation source (power below 20 mW) at energies in the range 830–850 nm, well below the SL's fundamental exciton absorption (~ 1.6 eV $= 775$ nm) and GaAs gap (1.515 eV $= 820$ nm) in order to avoid parasitic luminescence. The spectra were acquired using a triple subtractive configuration with spectral resolution around 0.1–0.2 cm^{-1}.

We show in Fig. 4 a typical experimental spectrum in the spectral range corresponding to the first zone-center acoustical folded-phonon minigap and obtained with laser wavelength $\lambda = 833$ nm. The *optical* cavity mode linewidth, determined mainly by the collection solid angle ($f/2.5$ optics) and the laser spot diameter, was around 10–12 cm^{-1}. This implies that no peak is selectively amplified, and thus that the relative intensity of the different spectral features is intrinsic [2]. To display only the Raman contribution a weak luminescence Lorentzian background corresponding to the optical cavity mode was subtracted in the shown spectrum. Identical spectra were acquired from different spot positions and with varying laser energies. A main peak centered at ~ 15 cm^{-1} is observed, together with secondary lines and oscillations. In Fig. 4 we also show for comparison the calculated Raman curve corresponding to the nominal structure. The agreement with the experimental curve is remarkable *without any adjustable parameter*. This includes the observation of the sought phonon-cavity mode, but also almost every other detail of the spectra. In fact, the only apparent difference is the predicted (and nonobserved) splitting of the peak in the low energy side of the phonon minigap (~ 14.3 cm^{-1}). This latter peak corresponds to the (-1) component of the zone-center doublet, mainly determined by the FS contribution (see Fig. 2). Its detailed shape is strongly dependent on the

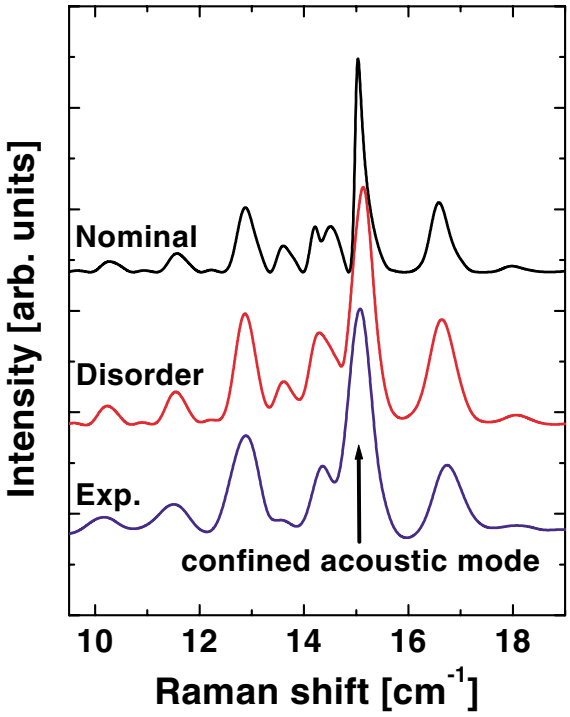

FIG. 4 (color online). Experimental Raman spectrum in the spectral range corresponding to the acoustical folded-phonon first center-zone minigap (Exp), obtained with laser wavelength $\lambda = 833$ nm. Also shown are calculated Raman curves corresponding to (i) the nominal structure (Nominal), and (ii) a phonon cavity with random disorder $\pm 4\%$ of the SL layer's thickness (Disorder).

interference between the FS and BS terms. As we will show next, the nonobservation of the peak splitting can be understood as being due to a small but expectable disorder due to interface roughness.

We have considered three possible mechanisms to account for the nonobservation of the above discussed FS peak splitting, namely, (i) differences of the real structure phonon-cavity spacer width with respect to the nominal value, (ii) destructive interferences in the Raman cross section originated in differences of the widths of the two (otherwise perfect) SL's [13], and finally (iii) interface roughness leading to width variations around the nominal value for all the layers making the two SL's. We found that only the last choice can explain the observed spectra with reasonable values of disorder. This is shown in Fig. 4, with a curve obtained by adding 300 spectra corresponding to phonon cavities with SL layer widths with random disorder $\pm 4\%$ around the nominal values. This corresponds to changes of ± 2.8 Å, or ± 1 GaAs or AlAs atomic monolayers at the interfaces. All peaks besides the 14.3 cm^{-1} line are quite stable to this disorder, and thus do not change except for a line broadening which reproduces almost exactly the measured spectral widths. The splitting of the 14.3 cm^{-1} peak, on the other hand, is washed out in correspondence with the experiment. In fact, as is clear from Fig. 4 the agreement between theory and experimental results is striking when the interface roughness is taken into account. This agreement includes the observation of all the main lines and most of the weaker oscillations, their spectral positions, and peak widths.

In conclusion, we have proposed a phonon cavity that displays novel confined acoustical excitations. In addition, we showed through photoelastic model calculations that these vibrations can be generated and probed by Raman scattering experiments that exploit the enhancement and confinement of photons in optical microcavities. Last, we fabricated a phonon cavity embedded within an optical microcavity based in GaAs and AlAs materials, and succeeded in observing the cavity-confined high frequency hyper-sound mode. Calculations that take into account a small but expectable interface roughness are able to account precisely for every detail of the observed spectra. The confined phonon modes in a phonon cavity are spatially localized highly monoenergetic excitations. These features open the way to studies of phonon stimulation, coherent phonon generation, and modified (enhanced or inhibited) electron-phonon interactions in phonon cavities. The confinement and enhancement of photons in an optical microcavity can be exploited, in addition, for the optical generation of these confined phonon modes.

[1] *Confined Electrons and Photons: New Physics and Applications*, edited by E. Burstein and C. Weisbuch (Plenum, New York, 1995).
[2] A. Fainstein *et al.*, Phys. Rev. Lett. **75**, 3764 (1995).
[3] A. Fainstein *et al.*, Phys. Rev. Lett. **86**, 3411 (2001).
[4] E. B. Tucker, Phys. Rev. Lett. **6**, 547 (1961).
[5] H. Haken, *Quantum Field Theory of Solids: An Introduction* (North-Holland, Amsterdam, 1976), p. 218.
[6] P. A. Fokker *et al.*, Phys. Rev. B **55**, 2925 (1997).
[7] See, e.g., T. Dekorsy, G. C. Cho, and H. Kurz, in *Light Scattering in Solids VIII*, edited by M. Cardona and G. Güntherodt (Springer, Heidelberg, 2000), p. 169.
[8] B. Jusserand and M. Cardona, in *Light Scattering in Solids V*, edited by M. Cardona and G. Güntherodt (Springer, Heidelberg, 1989), p. 49.
[9] V. Narayanamurti *et al.*, Phys. Rev. Lett. **43**, 2012 (1979).
[10] P. V. Santos *et al.*, Phys. Rev. B **36**, 4858 (1987).
[11] S. Adachi, J. Appl. Phys. **58**, R4 (1985).
[12] M. Trigo *et al.* Phys. Rev. B **66**, 125311 (2002).
[13] M. Giehler *et al.*, Phys. Rev. B **55**, 7124 (1997).
[14] P. X. Zhang *et al.*, Can. J. Phys. **70**, 843 (1992).